Journal of Solid State Chemistry **153,** 248–253 (2000)
doi:10.1006/jssc.2000.8748, available online at http://www.idealibrary.com on IDEAL®

High-Pressure Phase Transition in Cs_2KMnF_6

Y. Xu, K. Söderberg, and R. Norrestam[1]

Structural Chemistry, Arrhenius Laboratory, Stockholm University, S-106 91 Stockholm, Sweden

Received January 19, 2000; in revised form April 12, 2000; accepted April 20, 2000; published online July 17, 2000

The stability of the cubic high-temperature (HT) form of Cs_2KMnF_6, with an elpasolite structure, is studied at elevated pressures. The present study shows that the HT form of Cs_2KMnF_6 undergoes a pressure-induced phase transition at 40 kbar to a more ordered high-pressure (HP) phase of lower symmetry. The space group symmetry of the HP phase, *I4/mmm*, is the same as that observed for the low-temperature (LT) phase. High-pressure studies performed on the LT phase indicated no transitions up to 50 kbar and gave compressibility features similar to those obtained for the HP phase. Single-crystal *X*-ray diffraction data for the HP phase were collected at 44 kbar. Refining nine structural parameters against 69 independent significant reflections gave a linear R value of 0.072 ($wR = 0.086$). The values of the positional parameters are in agreement with those observed for the LT phase under ambient conditions. The transition characteristics for the HT form depend on the crystal quality and/or the pressure transmitting media used. With liquid argon, loaded into the pressure cell at low temperature and ambient pressure, the transition pressure became 30 kbar. With methanol:ethanol:water, loaded under ambient conditions, the transition was observed at 40 kbar.

Key Words: **single-crystal study; Mn^{3+} elpasolite; phase transition.**

INTRODUCTION

Recent studies in this laboratory (Xu, Carlson, Sjödin, and Norrestam (1)) showed that Cs_2KMnF_6 is polymorphic and adopts a tetragonal elpasolite low-temperature (LT) structure when quenched from below 530°C, while a cubic high-temperature (HT) phase is obtained by quenching from well above this temperature. If the structure of the LT phase is described by the nonconventional *F*4/*mmm* symmetry, an *a*:*c* ratio of 0.97 is obtained, indicating that the structure is pseudocubic.

The phase transition from the LT to the HT form originates from the directional disorder of the Jahn–Teller distortion around the Mn^{3+} ion. When hydrostatic pressure is applied to such a structure, constraints are imposed on the structure, yielding a more efficient packing. On this basis it seemed likely that the cubic HT phase would undergo a pressure-induced transition to a high-pressure (HP) phase with ordered distortions, and that the HP phase would be closely related to the LT phase.

The present study was undertaken to find out whether the high-temperature form of Cs_2KMnF_6 exhibits a pressure-induced phase transition and whether the transition is reversible, and also to determine the structure of a the new high-pressure phase if formed. This work is part of a research project concerned with structural studies of transition metal fluorides, particularly those containing Jahn–Teller distortions, at different pressures and temperatures.

EXPERIMENTAL

Synthesis. The LT form of Cs_2KMnF_6 was prepared by heating a mixture with the composition $2CsF + KF + MnF_3$, at elevated pressure. The mixture was put into a gold ampoule, which was sealed and inserted into a stainless steel container. The steel container was then filled with water and heated to 520°C at an external pressure of 2.5 kbar. To obtain the HT form, an LT specimen was put into a platinum tube, which was sealed and inserted into a quartz ampoule. The quartz ampoule was then evacuated, sealed, and heated to 600°C for 24 h, after which it was rapidly quenched in cold water.

High-pressure studies. A Merrill–Basset type of diamond anvil cell (DAC) (Diacell Products Uxor cell, 600 μm culet diameter) fitted with an Inconel gasket of thickness ≈ 400 μm, was used for the high-pressure studies. The gaskets were preindented between the diamond anvils before a hole of ≈ 300 μm diameter was drilled in the center of each one with an electroerosion device (Betsa, MH20 system). The cubic HT form of Cs_2KMnF_6 was studied with two different pressure transmitting media. In studies involving argon as transmitting medium, the DAC was filled by placing it, almost closed (< 0.1 mm opening distance),

[1] To whom correspondence should be addressed.

0022-4596/00 $35.00

under liquid argon for a few minutes. The cell was then closed, still under liquid argon. The compressibility of the tetragonal LT form of Cs_2KMnF_6 was measured with pentane:isopentane (1:1) as the pressure medium. X-ray powder patterns of Cs_2KMnF_6 were recorded from well-ground samples filled into gasket holes with diameters of ≈ 200 μm, also with pentane:isopentane (1:1) as the pressure medium.

Pressures in the DAC were estimated from fluorescence wavelength shifts observed from small (< 20 μm) ruby crystals located close to the specimen. Radiation was supplied by a 25 mW Ar ion laser, and the fluorescence shift was determined with a spectrograph equipped with an array detector, controlled by a personal computer. Pressure values were estimated with the proportionality constant, $2.74\ \mathrm{GPa \cdot nm^{-1}}$, given by Piermarini *et al.* (2). Pressure values were determined several times before and after the diffractometer investigations, to ensure that any changes in pressure which occurred during data collection could be neglected.

X-ray studies. The synthetic products were examined by Guinier X-ray powder techniques. The powder diffraction patterns of the prepared HT specimen of Cs_2KMnF_6 show that the major phase obtained was the cubic HT form. However, pure HT specimens could not be obtained by the synthetic procedures used. Conventional single-crystal photographic techniques were utilized to find suitable crystals of Cs_2KMnF_6 for the high-pressure experiments.

Single-crystal X-ray data were collected with a four-circle diffractometer (Siemens P4/RA) using Mo$K\alpha$-radiation ($\lambda = 0.71073$ Å). X rays were produced with a rotating anode X-ray generator operated at 5.0 kW with a filament size of 0.3×3 mm, and a collimator with an inner diameter of 0.3 mm. Unit cell parameters at different hydrostatic pressures (Table 1 and Fig. 1) were refined from 20 well-centered and well-distributed reflections in the reciprocal space ($13^\circ < 2\theta < 27^\circ$), at pressures up to about 50 kbar.

X-ray diffraction intensity data for the new HP phase were collected at 44.4(6) kbar with methanol:ethanol:water as the pressure medium. The data obtained were consistent with the same tetragonal space group symmetry, $I4/mmm$, as that of the low-temperature form of Cs_2KMnF_6. Intensities for 232 reflections with $2\theta < 80^\circ$ were collected. These reflections were not completely absorbed by the DAC equipment over a suitable range of the azimuthal angle ψ. The intensities were measured at those ψ values that gave a minimum in the absorption (shortest path lengths) by the diamonds and the beryllium plates of the DAC. The selection of reflections and the choice of best ψ values were performed by a set of C-programs written by one of the authors (R.N.). Least-squares refinements, with the structure of the LT phase as the initial model, and using nine parameters (two variable positional parameters) converged smoothly for 69 significantly observed unique reflections to an R value of 0.072 ($wR = 0.086$). To keep the number of refined parameters down, anisotropic thermal displacement parameters were allowed only for the Cs, while the K, Mn, and F atoms were treated as isotropically vibrating.

TABLE 1
Cell Parameters for KCs_2MnF_6 at Various Pressures

Pressure (kbar)	a (Å)	c (Å)	Volume (Å^3)	Width (°)
	Cubic Start Phase, MeOH:EtOH:Water			
Ambient	9.067(1)		745.4(2)	0.31(1)
2.0	9.060(2)		743.7(4)	0.41(1)
8.5	9.005(2)		730.2(4)	0.44(1)
21.1	8.907(3)		706.6(6)	0.45(1)
27.4	8.869(2)		697.6(5)	0.54(1)
33.1	8.825(5)		687.3(11)	0.54(1)
36.9	8.800(6)		681.4(15)	0.61(2)
41.6	8.730(5)	8.936(7)	681.0(10)	1.36(3)
45.5	8.708(5)	8.917(8)	676.2(10)	1.53(4)
51.3	8.696(6)	8.908(13)	673.6(12)	1.82(7)
37.2	8.741(6)	8.960(9)	684.6(11)	1.52(5)
29.0	8.788(4)	9.002(13)	695.2(10)	1.51(3)
24.9	8.816(5)	9.010(14)	700.3(11)	1.43(3)
18.4	8.874(4)	9.058(8)	713.3(7)	1.33(3)
11.5	8.921(4)	9.115(9)	725.4(8)	1.25(3)
	Cubic Start Phase, Argon			
1.9	9.055(6)		742.4(8)	0.30(3)
5.5	9.021(8)		734.1(11)	0.29(3)
17.0	8.948(1)		716.4(3)	0.31(2)
24.1	8.905(2)		706.2(4)	0.28(2)
33.3	8.769(3)	9.000(3)	692.1(6)	0.42(2)
41.8	8.716(1)	8.966(1)	681.1(2)	0.33(2)
47.6	8.678(3)	8.940(2)	673.3(5)	0.40(2)
38.4	8.732(2)	8.987(2)	685.2(4)	0.38(2)
35.3	8.752(3)	8.993(3)	688.8(5)	0.37(2)
12.9*	8.976(2)		723.2(4)	0.41(2)
28.7*	8.863(2)		696.2(4)	0.54(3)
39.0*	8.780(4)		676.8(8)	1.35(7)
45.1*	8.752(7)		670.4(9)	1.69(10)
50.6*	8.713(13)		661.5(17)	1.76(13)
	Tetragonal Start Phase, Pentane: Isopentane			
Ambient	8.936(2)	9.257(2)	739.2(3)	0.39(2)
14.2	8.851(1)	9.137(4)	715.8(3)	0.55(1)
20.9	8.822(5)	9.088(6)	707.3(7)	
27.0	8.780(5)	9.055(7)	698.0(8)	
27.8	8.774(5)	9.052(6)	696.8(7)	
36.4	8.726(6)	9.021(7)	686.9(9)	
38.5	8.703(4)	9.021(5)	683.3(6)	
44.4	8.675(4)	8.986(5)	676.2(6)	
50.0	8.660(4)	8.951(8)	671.3(7)	

Note. The esds of the pressures are about 0.6 kbar; the other esds are given within parentheses. The last column contains the average value of the estimated full ω width of the reflections used for cell determination. For each set of data the initial phase type and the pressure medium used are given. Measurements indicated with asterisks were performed on a crystal that had already once been subject to a phase transition. To facilitate the comparison between the cubic and tetragonal phases, cell parameters of a nonconventional F-centered tetragonal cell are given.

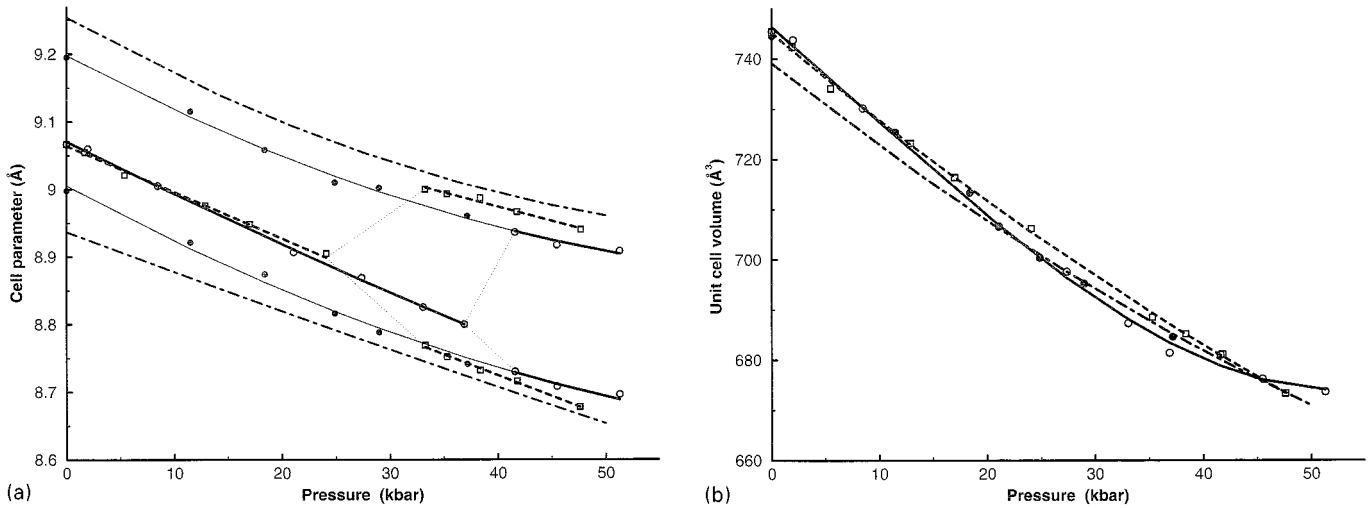

FIG. 1. (a) Unit cell parameters vs pressure and (b) unit cell volumes vs pressure. Measurements on the cubic high-temperature phase are denoted with squares for the results with argon as the pressure medium and with circles for those obtained with methanol:ethanol:water (16:3:1). Filled circles in the latter case denote decreasing pressure. Fitted curves are given as dashed lines and solid lines, respectively. For clarity, the results on the tetragonal low-temperature phase are only represented by fitted dot–dashed curves.

All structure refinements were made using the SHELXTL PC software package (3), with neutral atomic scattering factors from the *International Tables of Crystallography* (4). Geometric calculations were performed with the program PLATON (5), and the structure diagrams were made using the program ATOMS (6). Further experimental details for the X-ray data collections and structure refinements are shown in Table 2, and the values of the structural parameters obtained are given in Table 3. Bond distances are listed in Table 4.

TABLE 2
Experimental Details for the Structure Determinations at 44 kbar of Cs_2KMnF_6

Formula	Cs_2KMnF_6
Space group symmetry	*I*4/*mmm*
Formula units per unit cell, Z	2
Unit cell dimensions (Å), $T = 293$ K	$a = 6.126(2)$, $c = 8.981(3)$
Unit cell volume, V (Å^3)	337.0(2)
Pressure	44.4(6) kbar
Intensity data collection	ω–2θ scan
Maximum $\sin(\theta)/\lambda$ (Å^{-1})	1.3
Collected reflections	232
Unique reflections	82
Observed reflections ($\|F\| \geq 3\sigma_F$)	69
Absorption correction	Empirical
Structure refinement	Full-matrix, on $\sum\omega(\Delta F)^2$
Anisotropic displacement param	Cs
Number of refined parameters	9
Weighting scheme	$(\sigma_F^2 + 0.001F^2)^{-1}$
R for observed reflections	0.072
wR for observed reflections	0.086
Max. of $\|\Delta\|/\sigma$	< 0.001

Note. Data collection was performed using Mo$K\alpha$ radiation ($\lambda = 0.71073$ Å) at a temperature of 293 K. The esds are given within parentheses.

DISCUSSION

Cs_2KMnF_6 crystallizes with an elpasolite structure (cf. Fig. 2), which can be considered (7) as a lower symmetry variant of the cryolite structure adopted by, e.g., K_3AlF_6. The cryolite structure is closely related to the perovskite type structure and has a three-dimensional ReO_3-like framework of alternating corner-connected MnF_6 and KF_6 octahedra. The 12-coordinated Cs atoms are located in the cuboctahedral interstices formed by the octahedral net-

TABLE 3
Fractional Atomic Coordinates and Displacement Parameters (Å^2) with esds for Cs_2KMnF_6 at 44 kbar

Atom	x	y	z	u_{11}	u_{33}	U_{eq}
Cs	$\frac{1}{2}$	0	$\frac{1}{4}$	0.017(2)	0.028(2)	0.021(1)
Mn	0	0	0	—	—	0.026(4)
K	0	0	$\frac{1}{2}$	—	—	0.015(5)
F1	0.210(3)	0.210(3)	0	—	—	0.019(6)
F2	0	0	0.218(2)	—	—	0.022(9)

Note. Space group symmetry constraints on the displacement parameters imply that $u_{22} = u_{11}$ and $u_{23} = u_{13} = u_{12} = 0$.

TABLE 4
Bond Distances with esds in Tetragonal Cs_2KMnF_6 at Ambient Pressure (Low-Temperature Phase[a]) and at 44 kbar

Atoms	Multiplicity	Ambient	44.4 kbar
Cs–F1	8	3.240(4)	3.139(13)
F2	4	3.172(4)	3.076(20)
Mn–F1	4	1.860(6)	1.819(18)
F2	2	2.036(9)	1.958(18)
K–F1	4	2.609(6)	2.512(18)
F2	2	2.597(9)	2.533(18)

[a] Data from Ref. (1).

work. The packing pattern of the larger ions (Cs, K, and F) in two adjacent layers is shown in Fig. 2.

Cs_2KMnF_6 contains the Mn^{3+} ion, which, at the moderate ligand field strength exerted by the F^- ions, has a high-spin d^4 electron configuration. On removal of the degeneracy inherent in this configuration, distortion of the geometry of the MnF_6 coordination octahedra will occur (the stereochemical implication of the Jahn–Teller effect). The dominating distortion is an axial elongation of an octahedron, viz., a prolate distortion. A directional ordering of the axial distortions would then lower the space group symmetry, from cubic $Fm3m$ for an ideal elpasolite (K_2NaAlF_6), to tetragonal $I4/mmm$ for Cs_2KMnF_6 (low-temperature form). The ratio of the lengths of the two longer axial Mn–F bonds and the two shorter equatorial ones in the MnF_6 octahedra at ambient conditions is 2.036:1.860 = 1.095 with an esd of 0.006. The magnitude of the distortions is also reflected by the unit cell parameter ratio $c{:}a\sqrt{2}$ for the tetragonal LT phase, which is 1.0359(3). As the magnitudes of the distortions are limited, a disorder of the distortion directions will occur in the high-temperature form of Cs_2KMnF_6 (1). As a consequence of the disorder (see also Massa (8)) the symmetry becomes cubic ($Fm3m$) again, and symmetry constraints ensure that all Mn–F distances become virtually equal (1.931(5) Å). In this case the Mn–F distance represents a weighted average of the values for the "true" Mn–F bonds.

Dynamic Jahn–Teller effects could also lead to a similar situation being observed. Both these models should give high values for the thermal displacement factors of the F^- ions. In our previous study under ambient conditions, the displacement parameters of the fluorine atoms in the cubic phase were about twice those observed for the tetragonal phase (0.022 $Å^2$ and 0.042 $Å^2$, respectively).

The ratio $c{:}a\sqrt{2}$ remains constant (1.04) when the hydrostatic pressure is increased from ambient to 44 kbar. This would suggest that the axial distortions of the MnF_6 octahedra are unaffected by pressure. The ratio between the

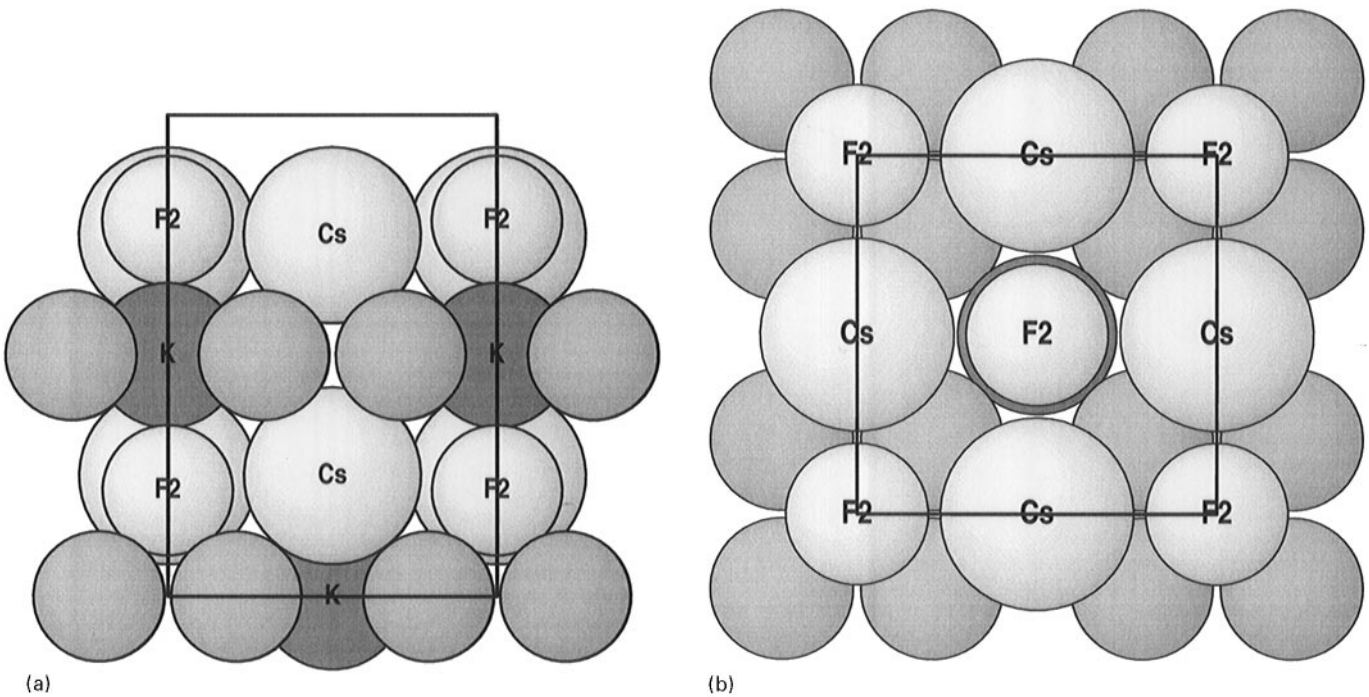

FIG. 2. Packing pattern of the larger Cs^+, K^+, and F^- ions in Cs_2KMnF_6. (a) View along [0 1 0], with [1 0 0] horizontal and [0 0 1] vertical, and (b) view along [0 0 1], with [1 0 0] horizontal and [0 1 0] vertical. For clarity the positions of the F1 fluorine atoms, drawn as smaller gray circles, are not labeled. The origin is at the lower left corner.

two longer axial Mn–F bond lengths and the four shorter equatorial ones decreases from 1.095(6) at ambient pressure to 1.076(13) at 44 kbar. However, in view of the esds of the ratios the decrease is only significant to a confidence level of 85%.

Studies of the HT form of Cs_2KMnF_6 were carried out with two different pressure transmitting media to see if the observed phase transition was dependent on the medium used. The two media chosen were methanol:ethanol:water in the ratio 16:3:1 and liquid argon. The results obtained were slightly different (Table 1 and Fig. 1). Thus, with the methanolic pressure medium a nonreversible transition from the cubic HT form to the tetragonal HP form was observed at about 40 kbar. With liquid argon the transition occurred at a 10 kbar lower pressure. It should also be noted that the cell parameters observed for the HP forms became slightly different. Those observed with liquid argon are closer to those of the tetragonal LT form. More astonishing was that with argon the transition was reversed from tetragonal back to cubic when the pressure was lowered from 35.3 kbar to 12.9 kbar.

Various reasons can be proposed for this difference in behavior, including the possibility that the small interactions between the media and the crystal differ. The two pressure media might also have slightly different nonisostatic properties, and in this connection it should also be noted that argon crystallizes already below 20 kbar. Another reason for this variation in behavior could be connected with the increase in mosaicity expected to occur when the temperature of the DAC was lowered to the boiling point of liquid nitrogen in order to fill the pressure chamber of the DAC with liquid argon. However, the observed widths ($\Delta\omega \approx 0.3^\circ$) of the reflections (Table 1) before the transition were significantly smaller in the argon experiments than in the methanol experiments ($\Delta\omega \approx 0.45^\circ$), which suggests that the crystal quality (or rather the translation symmetry) was more perfect for the crystal used in the argon experiments. The reflection widths after the transition were still significantly smaller in the argon experiments ($\Delta\omega \approx 0.3$–0.4°) than in the methanol experiments ($\Delta\omega \approx 1.3$–1.8°).

Some general comments on the relevance of crystal quality and other crystal characteristics for observing different transition pressures have been made by Sowa *et al.* (9) in connection with high-pressure studies of KPF_6. The present study is focussed on studies of the pressure-induced ordering of the Jahn–Teller distortions in the cubic high-temperature form. Investigations into the existence of any low-temperature transitions, that also might affect the crystal characteristics, were accordingly considered to be outside the scope of the present study. It is noteworthy that the closely related compound Rb_2KScF_6, structurally investigated by neutron powder techniques, shows three allotropic forms (Faget *et al.* (10)). In addition to a cubic elpasolite form above 252 K and a tetragonal form in the region between 223 and 252 K, a third monoclinic form is stable below 223 K. This monoclinic form has a cryolite-type related structure. The Sc^{3+} ions with their d^0 configuration have in general an effective spherical shape compared to the general ellipsoidal shape (11) of the Mn^{3+} ions with d^4 configuration. Thus, the presence of Mn^{3+} ions in the present study of KCs_2MnF_6, with their pronounced property to stabilize a tetragonal distortion of MnF_6 octahedra, leads to a much larger thermal high-temperature stability range (up to over 800 K) for the tetragonal form. What happens if the stability range is extended also into the very low temperature region is, as discussed above, outside the scope of this paper.

As described above, with argon as pressure medium the transition could also be reversed once by lowering the pressure well below the transition point. When the crystal had been subject to two transitions (argon medium), to the HP form and back to the cubic form, by increasing the pressure and then lowering it again, no transition back to the HP form could be observed at pressures up to 50 kbar (observations marked with asterisks in Table 1). This "nonelastic" feature shows that the transition cannot be regarded as strictly reversible. Above 50 kbar the reflection intensities decreased rapidly and the widths ($\Delta\omega$) became so large (several degrees) that reliable centering of the reflection positions was no longer possible. To conclude, the observed characteristics of the transition might well depend on the crystal quality. A better crystal quality could lower the energy needed for the transition. However, the possibility that the transition is affected by the different features of the pressure transmitting media used cannot be neglected.

The observed compressiblities of Cs_2KMnF_6, as reflected by the change in unit cell volumes (Fig. 1b), for the different pressure media are well described by a Birch–Murnaghan type of equation of state (EOS),

$$P[x] = \frac{3}{2} K_0 (x^{-7/3} - x^{-5/3}),$$

where P is the pressure, $x = V/V_0$ the relative volume change, and K_0 the isothermal bulk modulus at zero pressure. With the EOS used it is implicit that the first pressure derivative (K_0) of the bulk modulus has a value of 4.00 in the pressure interval. Nonlinear least-squares determination of both the zero pressure bulk modulus K_0 and the unit cell volume V_0 were performed. The observed data for the cubic HT form were rather independent of the pressure medium used. The obtained values from the "methanol data" were $K_0 = 37.5(17)$ GPa and $V_0 = 745.4(18)$ Å^3, and those from the "argon data" 38.1(17) GPa and 745.9(5) Å^3, respectively. The experimental cell volume (745.4(2) Å^3) at zero pressure lies within two esds of the calculated ones. The tetragonal

LT form is slightly less compressible (cf. Fig. 1b); the values obtained were $K_0 = 42.3(6)$ GPa and $V_0 = 739.1(7)$ Å^3. Again, the calculated V_0 value agrees well with that observed, 739.2(3) Å^3.

Compounds containing Cs^+ as the only cation are much softer materials than Cs_2KMnF_6. The value of the bulk modulus for Cs_2CuCl_4 is 15.0(2) GPa (Xu *et al.* (12)), and for common Cs halides bulk moduli lie in the range 13 to 18 GPa (Hazen and Finger (13)). The rigid three-dimensional ReO_3 type of octahedral network in Cs_2KMnF_6, formed by alternating corner-sharing KF_6 and MnF_6 octahedra, offers an obvious explanation for the lower compressibility. The compressibility of Cs_2KMnF_6 is similar to that observed for Na_3MnF_6 ($K_0 = 47.8(6)$ GPa, Carlson *et al.* (14)) with its related ReO_3 network of NaF_6 and MnF_6 octahedra.

ACKNOWLEDGMENTS

The authors are indebted to the Swedish National Research Council for the financial support of the present research project. We are also grateful to Arne Sjödin (Stockholm University) for his assistance with the syntheses and to N. L. Arthur (La Trobe University, Melbourne) for his comments on the manuscript.

REFERENCES

1. Y. Xu, S. Carlson, A. Sjödin, and R. Norrestam, *J. Solid State Chem.* **150,** 399–403 (2000).
2. G. J. Piermarini, S. Block, J. D. Barnett, and A. Forman, *J. Appl. Phys.* **46,** 2774–2780 (1975).
3. *SHELXTL PC*, release 4.1, Siemens Analytical X-ray Instruments Inc., Madison, WI, 1990.
4. "International Tables of Crystallography," Vol. IV. Kynoch Press, Birmingham, 1974.
5. A. L. Spek, PLATON, Program for the analysis of molecular geometry,Univ. of Utrecht, Utrecht, The Netherlands, 1990.
6. E. Dowty, ATOMS, a computer program for displaying atomic structures, 521 Hidden Valley Rd., Kingsport, TN 37663, 1989.
7. A. F. Wells, "Structural Inorganic Chemistry," 5th Ed. Clarendon Press, Oxford, 1984.
8. W. Massa, *Z. Anorg. Allg. Chem.* **491,** 208–216 (1982).
9. H. Sowa, K. Knorr, F. Mädler, H. Asbahs, and A. Kutoglu, *Z. Kristallogr.* **214,** 542–546 (1999).
10. H. Faget, J. Grannet, A. Tressaud, V. Rodriguez, T. Roisnel, I. N. Flerov, and M. V. Gorev, *Eur. J. Solid State Inorg. Chem.* **33,** 893–905, (1996).
11. R. Norrestam, *Z. Kristallogr.* **209,** 99–106 (1994).
12. Y. Xu, S. Carlson, K. Söderberg, and R. Norrestam, *J. Solid State Chem.* **153,** 212 (2000).
13. R. M. Hazen and L. W. Finger, *J. Geophys. Res.* **84,** 6723–6728 (1979).
14. S. Carlson, Y. Xu, U. Hålenius, and R. Norrestam, *Inorg. Chem.* **37,** 1486–1492 (1998).